

Electronic Supplementary Information

Interaction potential surface between Raman scattering enhancing nanoparticles conjugated with a functional copolymer

Takeshi Morita,^{*a} Yuki Ogawa,^a Hiroshi Imamura,^b Kouki Ookubo,^c Nobuo Uehara^c and Tomonari Sumi^d

^a Department of Chemistry, Graduate School of Science, Chiba University, Chiba 263-8522, Japan

^b Department of Applied Chemistry, College of Life Sciences, Ritsumeikan University, Shiga 525-8577, Japan

^c Department of Material and Environmental Chemistry, Graduate School of Engineering, Utsunomiya University, Tochigi 321-8585, Japan

^d Research Institute for Interdisciplinary Science, Okayama University, Okayama 700-8530, Japan.

Theoretical Methods

Iteration procedure for the model-potential-free analysis.

An initial guess in the iterative calculation is given by the followings:

$$\hat{c}(q) = \hat{c}^{\text{HS}}(q), \quad (\text{A1})$$

$$\hat{\gamma}_s(q) = \hat{\gamma}_s^{\text{HS}}(q) = 0,$$

(A2)

$$\hat{h}_{\text{old}}(q) = \hat{h}^{\text{HS}}(q), \quad (\text{A3})$$

$$\hat{h}'(q) = \begin{cases} \hat{h}_{\text{exp}}(q) = [S_{\text{exp}}(q) - 1] & q \leq q_h \\ \hat{h}^{\text{HS}}(q) & q > q_h \end{cases}, \quad (\text{A4})$$

where $S_{\text{exp}}(q)$ is the experimental $S(q)$, and n_0 is the number density of the colloidal particle, and $\hat{h}^{\text{HS}}(q)$ is obtained from the hard-sphere reference system with n_0 . The iterative calculation is continued until the value of $S(q) = 1 + n_0 \hat{h}(q)$ is equal or very close to $S_{\text{exp}}(q)$ at a small q .

$$\text{Step 1} \quad \hat{c}^{\text{EX}}(q) = \hat{c}(q) - \hat{c}^{\text{HS}}(q). \quad (\text{A5})$$

$$\text{Step 2} \quad \hat{c}(q) = \hat{h}'(q) - [\hat{\gamma}_s(q) - \hat{c}^{\text{EX}}(q)]. \quad (\text{A6})$$

$$\text{Step 3} \quad \hat{\gamma}_s(q) = \hat{c}(q) / [1 - n_0 \hat{c}(q)] - \hat{c}^{\text{HS}}(q). \quad (\text{A7})$$

$$\text{Step 4} \quad \hat{\gamma}_s(q) = a \hat{\gamma}_s(q) + (1 - a) \hat{\gamma}_s^{\text{old}}(q), \text{ where } a \text{ is the dumping parameter.} \quad (\text{A8})$$

$$\text{Step 5} \quad \hat{\gamma}_s^{\text{old}}(q) = \hat{\gamma}_s(q). \quad (\text{A9})$$

$$\text{Step 6} \quad h(r) = \begin{cases} \exp[\hat{\gamma}_s(q) + BF(r)] - 1 & r > d_{\text{HS}} \\ -1 & r \leq d_{\text{HS}} \end{cases}. \quad (\text{A10})$$

Step 7 If a difference $|S(q) - S^{\text{old}}(q)|$ determined at n^{th} iterative calculation becomes larger than that determined at $(n-1)^{\text{th}}$ iterative calculation, where $S(q)$ and $S^{\text{old}}(q)$ are respectively calculated at n^{th} and $(n-1)^{\text{th}}$ iteration, go to step 8 (outside the loop of the iterative calculation); otherwise, we update $\hat{h}'(q)$ using Eq. (A11) and go back to step 1.

$$\hat{h}'(q) = \begin{cases} \hat{h}_{\text{exp}}(q) = [S_{\text{exp}}(q) - 1] / n_0 & q \leq q_h \\ \hat{h}(q) & q > q_h \end{cases}. \quad (\text{A11})$$

Step 8 $S(q)$ is calculated via $S(q) = 1 + n_0 \hat{h}(q)$ and $V(r)$ is calculated using

$$V(r) / k_B T = -\ln g(r) + [h(r) - c(r) + BF(r)]. \quad (\text{A12}).$$

Computational details.

To reproduce the experimental $S(q)$ for p(NIP-TETA) and p(NIP-DETA), we determined an optimal number density of the nanoparticle n_0 by varying it as a parameter. The introduced number density n_0 can be regarded as a local average density around each

nanoparticle. In contrast to n_0 , the total number density of the nanoparticle $\rho = N/V$ is suitably low so that the particle-particle interference effect is negligible in the absence of the functional copolymers. The self-assembly of the nanoparticles is caused by adding the functional copolymers p(NIP-TETA) and p(NIP-DETA) into the diluted nanoparticle solution, resulting in a local increase in the number density around a nanoparticle. In the present analysis, we introduced such a local average density n_0 to determine the local density distribution around a nanoparticle $n(r) = n_0 g(r)$ from the experimental $S(q)$. Note that the obtained $n(r)$ or $g(r)$ includes no correlations between aggregated clusters that could be observed by ultra-small-angle X-ray scattering. However, this is not problematic in our purpose of the present analysis, since we focus on local self-assembled structures between the nanoparticles, which are connected with the UV-vis spectra and the surface-enhanced Raman scattering. In addition, for convenience in the present analysis, we extrapolated the experimental scattering intensity $I(q)$ in the small-angle region where we have no SAXS data. $I(q)$ for the nanoparticle solutions without the functional copolymers, namely, $I_0(q)$, which was used as the form factor $|F(q)|^2$, was extrapolated using the Guinier approximation, while $I(q)$ for the nanoparticle solutions conjugated with the functional copolymers p(NIP-TETA) and p(NIP-DETA) was extrapolated using a Lorentz function. The experimental $S(q)$ s shown in Fig. S1 were determined using $S(q) = I(q)/I_0(q)$. The obtained raw values for $S(q)$ s were dealt with a smoothing. The integral equation described above was solved without the bridge function $BF(r)$. The maximum radial distance is 300 nm, which is discretized by 4096 grid points. We used 1.07 nm^{-1} and 1.11 nm^{-1} as q_h (see Eq. A11) for p(NIP-TETA) and p(NIP-DETA), respectively. The optimal local average number densities n_0 for p(NIP-TETA) and p(NIP-DETA) at 298 K are $3.0 \times 10^{-5} \text{ nm}^{-3}$ and $1.32 \times 10^{-5} \text{ nm}^{-3}$, respectively.

$S(q)$ s obtained from the MPF analysis agreed well with the experimental $S(q)$ s as seen in Figs. S1a and S1b. The radial distribution functions $g(r)$ s corresponding to the theoretical $S(q)$ s are shown in Fig. S1c. The extrapolation of $I(q)$ and $I_0(q)$ gives a small-angle peak in $S(q)$ for p(NIP-TETA) as shown in Fig. S1a. Fig. S1d provides $g(r)$ enlarged at the distances corresponding to the small-angle peak position in $S(q)$ of p(NIP-TETA) seen in Fig. S1a, indicating that this small-angle peak is the reflection of the long-ranged slight density fluctuation at the distances between 60 and 150 nm. The validity of the prediction by the present analysis should be assessed by SAXS measurement including much more

smaller-angle region. However, the existence does not affect our discussion on the surface-enhanced Raman scattering.

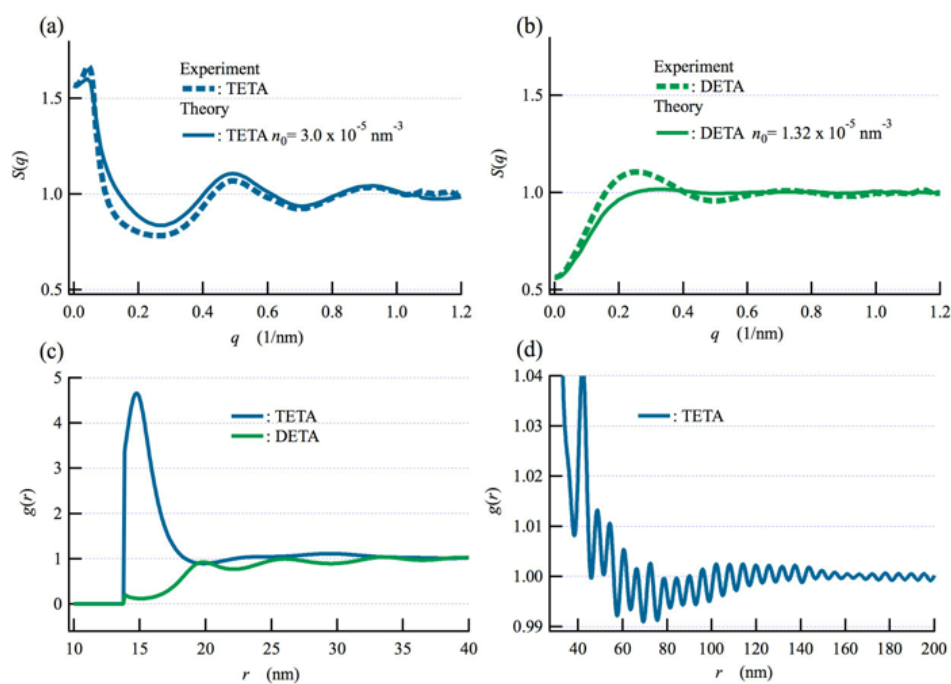


Fig. S1. Comparison of the theoretical $S(q)$ s with the experimental $S(q)$ s. (a) p(NIP-TETA) with $n_0 = 3.0 \times 10^{-5} \text{ nm}^{-3}$. (b) p(NIP-DETA) with $n_0 = 1.32 \times 10^{-5} \text{ nm}^{-3}$. (c) The radial distribution function $g(r)$ obtained for p(NIP-TETA) and p(NIP-DETA). (d) $g(r)$ enlarged at the distance corresponding to the small-angle peak position in $S(q)$ of p(NIP-TETA) as seen in Fig. S1a.